ELSEVIER

Materials Science and Engineering A 415 (2006) 45–52

MATERIALS SCIENCE & ENGINEERING A

www.elsevier.com/locate/msea

Kinetic spraying deposition behavior of bulk amorphous NiTiZrSiSn feedstock

Sanghoon Yoon [a], Changhee Lee [a,*], Hansin Choi [b], Hyoungho Jo [b]

[a] *Division of Materials Science & Engineering, College of Engineering, Hanyang University 17 Haengdang-dong, Seongdong-ku, Seoul 133-791, Republic of Korea*

[b] *Nanomaterial Team, Advanced Materials R&D Center, Korea Institute of Industrial Technology, Incheon 406-130, Republic of Korea*

Received in revised form 2 August 2005; accepted 10 August 2005

Abstract

A kinetic spraying process, which is basically a solid-state deposition process, was used for the formation of a fully amorphous coating. By using a pre-heating system for the powder carrier gas and using helium for the process gas, it was possible to form an amorphous coating. The main process parameters evaluated during this study were gas species [N_2 and He] and pre-heating temperature [RT (below T_g) and 550 °C (liquid metallic region)]. Aside from the empirical approach, in-flight particle velocity within the kinetic spraying process was measured using a SprayWatch-2i system. The deposition behavior of a NiTiZrSiSn bulk amorphous powder was observed when it was sprayed using the kinetic spraying process. In order to predict the temperature-dependent deformation behavior of the bulk amorphous material during impact, Vickers microhardness, as an indirect method, was measured at various temperatures.

While the bulk amorphous feedstock material was being coated, both the kinetic and thermal energies of the in-flight particles were important. The former affected the deposition of the bulk amorphous coating, while the latter had more effect on the mechanical properties of the coating. Particle deposition behavior was considered from the viewpoint of the environmental effect, such as particle–energy combination, on the deposition behavior. The bonding of the impacting NiTiZrSiSn bulk amorphous particle was primarily caused by temperature-dependent deformation and fracture (local liquid formation) behavior.

Keywords: NiTiZrSiSn bulk metallic glass; Kinetic spraying; In-flight particle energy; Deposition behavior

1. Introduction

Because of the unique material properties of bulk metallic glasses, the possibilities for their structural applications have been investigated extensively [1–3]. Though they show high specific strength and hardness, low friction coefficient, and superior resistance to localized corrosion [3], the catastrophic nature of their failures still limits their industrial applications [4,5]. Therefore, various kinds of hybrid materials have been suggested in order to enhance ductility. Coating technology is considered to be the most effective method for producing two-dimensional hybrid materials, especially for hard and brittle materials. Too chatty, the effects of thermal energy and oxidation behavior of the in-flight bulk metallic glass particle on the microstructural evolutions of the as-sprayed coatings were investigated in vacuum and atmospheric plasma spraying and high-velocity oxy-fuel spraying processes [6,7]. Both thermal and chemical instability deteriorate the glass-forming ability of the bulk metallic glass [8]. Considering the susceptibilities of bulk metallic glass feedstock to thermally activated processes, such as crystallization and oxidation, the kinetic spraying process was chosen to form a uniform, amorphous overlay. The deposition of individual particles is largely dependent on their kinetic energy and the impact behavior. Impacting particles need to have sufficient kinetic energy to develop intimate contact between splat and substrate and between splats during kinetic spraying. Unlike other metallic materials commonly used in engineering application, bulk metallic glass materials exhibit unique mechanical properties that depend on temperature and strain rate [4,5,9–12]. With respect to temperature dependence, the deformation behavior can be divided into two parts according to the temperature: bulk metallic glass deforms inhomogeneously below the glass transition temperature through localized shear band formation [9–12]. Meanwhile, so-called superplasticity is achieved by heating the

* Corresponding author. Tel.: +82 2 2220 0388; fax: +82 2 2293 4548.
E-mail address: chlee@hanyang.ac.kr (C. Lee).

0921-5093/$ – see front matter © 2005 Elsevier B.V. All rights reserved.
doi:10.1016/j.msea.2005.08.132

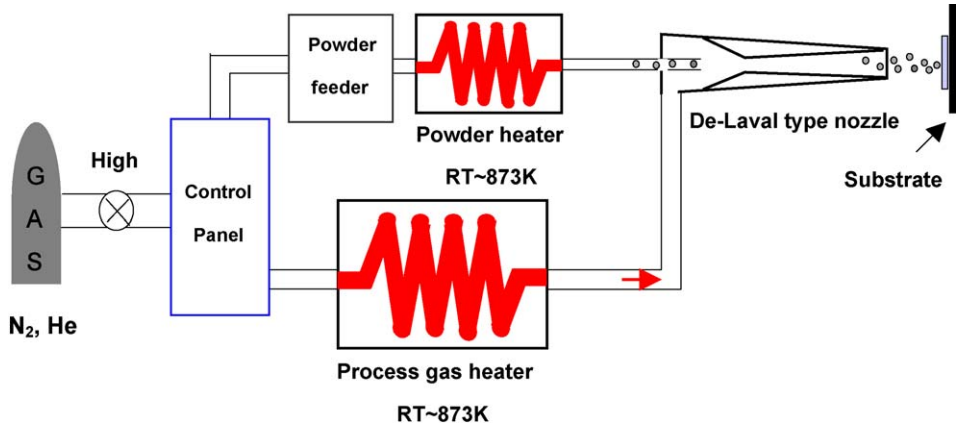

Fig. 1. Layout of modified kinetic spraying system.

Table 1
Process parameters

Designation	Gas	Process gas		Carrier gas temperature	Parameter held constant
		Pressure (MPa)	Temperature (°C)		
NL	Nitrogen	2.9	600	RT	
NH				550 °C	Spray distance: 30 mm; feeding rate:
HL	Helium			RT	4 rpm(36 g min^{-1}); gun travel rate: 0.01 m s^{-1}
HH				550 °C	

bulk metallic glass within the supercooled liquid region where the viscosity is markedly lower. Generally, the sudden decrease of the flow stress is observed at temperatures of about two-thirds of the melting point. From the viewpoint of impact engineering, heat is generated by friction and deformation during impact and is dissipated by thermal conduction. Accordingly, the heat balance achieved by the heat generation rate and the dissipation rate affects the thermomechanical properties of impacting particles. When the strain rate is high, as generated during kinetic spraying, the heat is adiabatically generated and reduces the flow stress for deformation, which is known as adiabatic shearing [13]. In order to facilitate the transition to adiabatic shearing, the kinetic spraying system was modified as shown in Fig. 1. For the conventional kinetic spraying system, the working gas is fed into a gas control unit and is separately supplied as process gas and powder carrier gas. In order to increase the gas velocity, the process gas is generally heated, but the powder carrier gas is generally not heated. In this situation, the injected particles can be heated during the limited time they reside within the nozzle. On the other hand, it can be expected that the in-flight particle temperature will be much higher when an additional heating system is used as shown in Fig. 1. In this study, the bulk metallic glass particle deposition behavior and the coating formation were investigated from both the kinetic energy and thermal energy viewpoints. To do this, working gas species and additional heating were chosen for the process parameters as shown in Table 1.

2. Experimental work

NiTiZrSiSn bulk metallic glass feedstock was manufactured using an inert gas atomization method [11]. Before spraying, the as-atomized particles were sieved to obtain a feedstock with particle sizes below 45 μm (−45 μm + 5 μm). Phase, size, morphology, and thermal properties of the feedstock were investigated using X-ray diffractometry, laser scattering, scanning electron microscopy, and differential scanning calorimetry (SDT Q 600), respectively. For the differential scanning calorimetry, particles were heated at a rate of 0.167 K s^{-1} within an inert argon gas environment. Mild steel substrates were finely polished for enhancing individual particle deposition but grit-blasted for coating formation. The size of the substrate was 50 mm × 70 mm. Process parameters are listed in Table 1. Other parameters were kept constant except for the process gas species and the powder carrier gas temperature. Powder feed rate was as low as possible (<5 g min^{-1}) for individual particle deposition studies, but was increased to 9 g min^{-1} for coating formation. In-flight particle velocity was measured by SprayWatch (which was manufactured by Oseir Ltd., Finland). A high speed camera (SprayWatch camera unit) was used to monitor the spraying processes. A laser device (HiWatch laser unit) was used for particle illumination. These two units were connected to a personal computer, which was used for system controlling, calculation, and display. The SprayWatch system mounting is shown in Fig. 2. The effective size of the measured region was 20 mm × 20 mm × 1 mm. The center of the measured region was 30 mm from the nozzle exit in the axes direction. A multi-pulse imaging technology was used in this system. During one exposure of the camera, three or more laser pulses were emitted (Fig. 3a). Then, the particle's stretch image was obtained, as shown in Fig. 3b. The particle velocity was calculated from the interval time of laser emission and the particle flying distance measured from the image, as shown in Fig. 3c. Splat morphol-

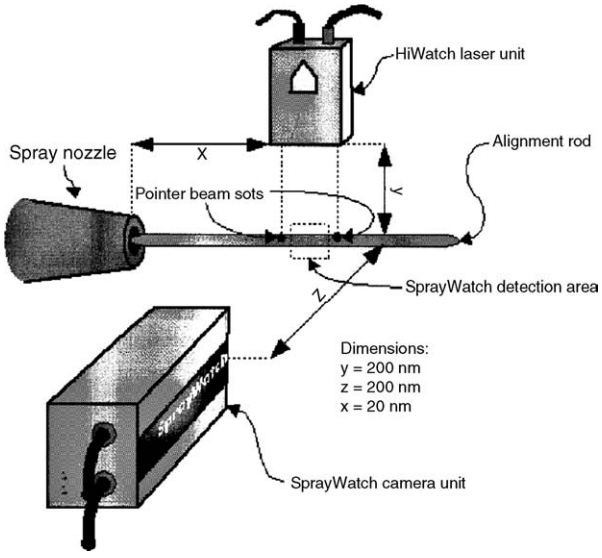

Fig. 2. Mounting of the SprayWatch system.

ogy was observed using a scanning electron microscope (JSW-6300) with an energy-dispersive spectrometer. Cross-sectional microstructures of the as-sprayed coatings were investigated and porosity was measured using image analysis (Image-Pro Plus 4.5). Phase composition of the overlays was also identified by X-ray diffraction. To measure the bond strength of coating/substrate, the Stud Pull Coating Adherence Test was carried out using a Romulus Bond Strength Tester. The coating specimens were cut into 10 mm × 12 mm squares. Aluminum test studs with a 2.70 mm diameter head and 12.5 mm length were attached on the coating surfaces, which were micro-polished with 0.3 μm alumina. The tests used a unique ultra-strong, non-stressing, thermally curing epoxy bonding agent (with ultimate strength higher than 85 MPa), which was already applied on the face of the studs. The test stud assemblies were placed in an oven and cured at 150 °C for 90 min. After a stud pull test, the bond strength could be evaluated.

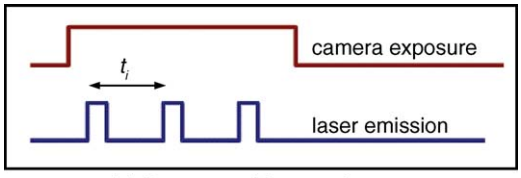

(a) Camera and laser action.

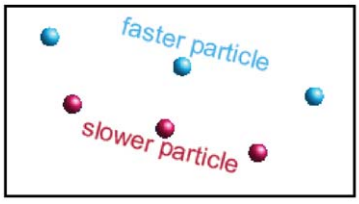

(b) Flying particles

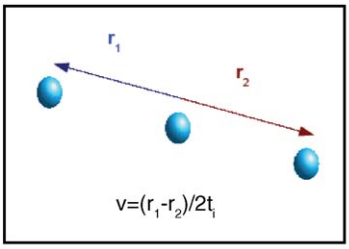

(c) The calculation of particle velocity

Fig. 3. Schematic of the SprayWatch system.

3. Results and discussion

3.1. Feedstock materials

Characteristics of the NiTiZrSiSn bulk metallic glass can be seen in Fig. 4. Spherical particles having a smooth surface resulted from the gas atomization process. The particle sizes varied from 5 μm to 45 μm, and the mean particle size was 25 μm. In the X-ray diffraction of the feedstock, a diffuse peak is shown in Fig. 4c, a typical diffraction pattern for an amorphous material. An endothermic heat flux corresponding to the glass transition was observed at 546 °C [T_g: glass transition temperature] and an exothermic one due to the onset of crystallization began at 597 °C [T_x: the onset point for the crystallization]. The supercooled liquid region [$\Delta T = T_x - T_g$] was 51 °C.

3.2. Individual particle deposition

Fig. 5 shows individual particle deposition behavior on a mild steel substrate as a function of the working gas species and carrier gas temperature. The deposition of bulk metallic glass particles onto steel was regarded as that of a hard and elastic particle on a soft and plastic substrate: Fig. 9a and b shows typical features of the bulk metallic glass particle and substrate combination when nitrogen was used as the process gas. It was difficult to locate individual bulk metallic glass splats on the substrate. Each bulk metallic glass particle (mainly small particles) was deeply embedded into the substrate by relaxing the impacting particle energy caused by the severe localized deformation of the substrate. In this case, the geometry between the impacting particle and the substrate seems to be a critical factor for splat formation and was largely dependent on the impact velocity and particle size. On the other hand, the ratio of the splat to the crater was markedly increased by changing the process gas to helium and was further increased by additional powder heating. Also, there was a significant change in the deposition behavior. It was evident that partial melting of bulk metallic glass occurred during impact (Fig. 5c and d) as indicated by the liquid jet at the interface between the bulk metallic glass splat and the substrate in (c) and mass flow on the crater in (d).

Fig. 6 shows the effects of carrier gas temperature on the impact behavior of a bulk metallic glass particle on a previously deposited splat. Particles without any additional heating exhibited severe fracture with notable shear bands [white arrows] on the surface, as shown in (a) and (b). Adiabatic melting was evident in the fractured particle as shown in the rectangular box in (b); this was the bonding mechanism of the bulk metallic glass in this situation. It could be deduced that the pressure building in the impacting splat resulted in fracture before softening and

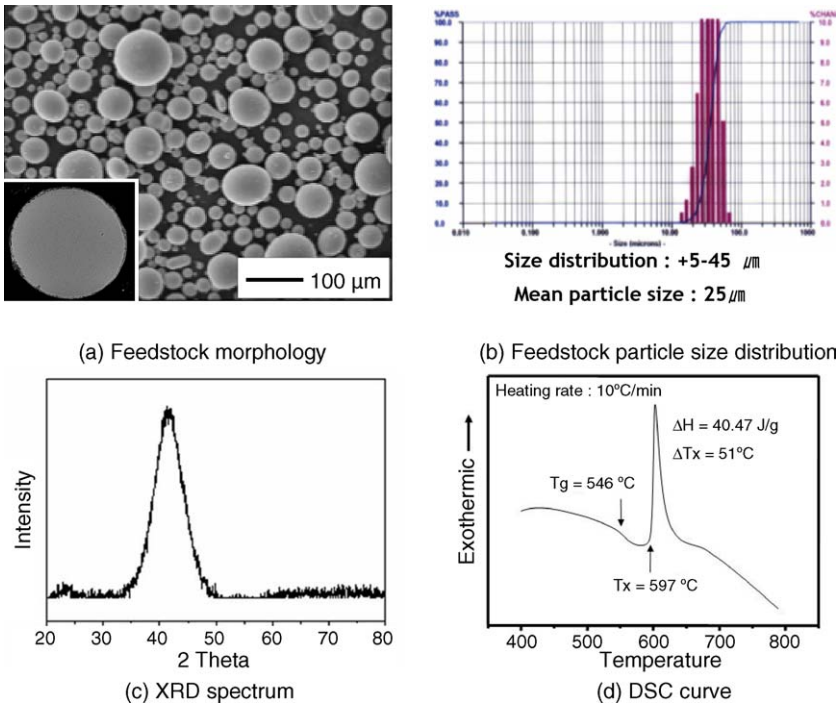

Fig. 4. Characteristics of the NiTiZrSiSn bulk metallic glass feedstock.

that the fracture caused melting, which is typical of the fracture behavior of bulk metallic glass [14–16]. The melt seemed to act as a binder for the deposition; however, severe deformation without any evidence of fracture was dominant for particles that were deposited using additional heating. In this case, adiabatic heat generation and softening occurred before the pressure reached the fracture strength because of the increased initial particle temperature at the moment of impact.

Three phenomena occurred when a particle with high kinetic energy impacted on a substrate, as shown in Fig. 7. Part A shows low (or no) deformation due to low stress during impact. The shear bands and fracture shown in part B were caused by high

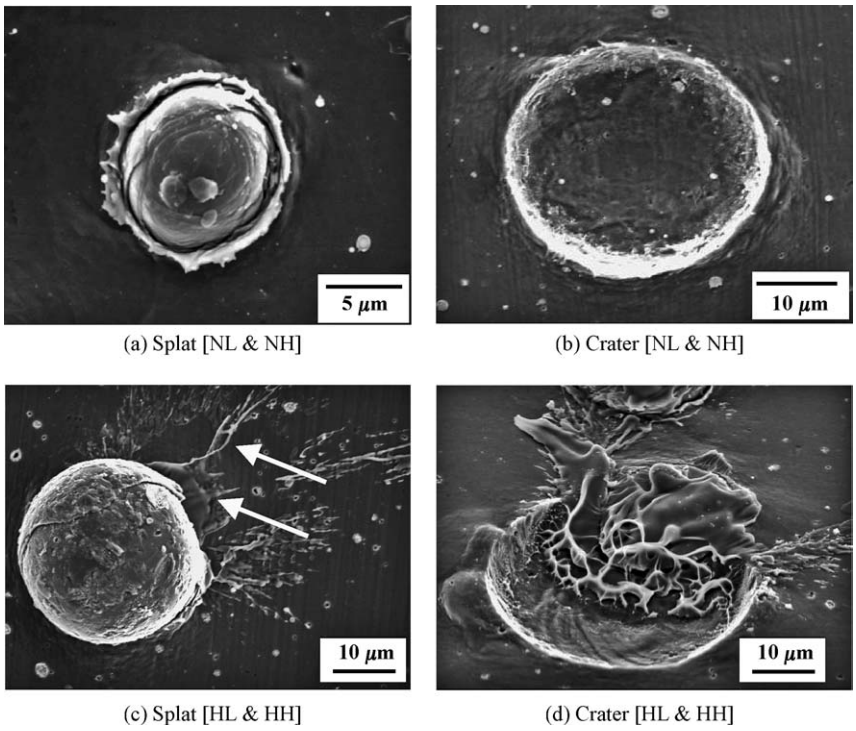

Fig. 5. Characteristic features of a splat on a mild steel substrate according to the process gas species and additional heating.

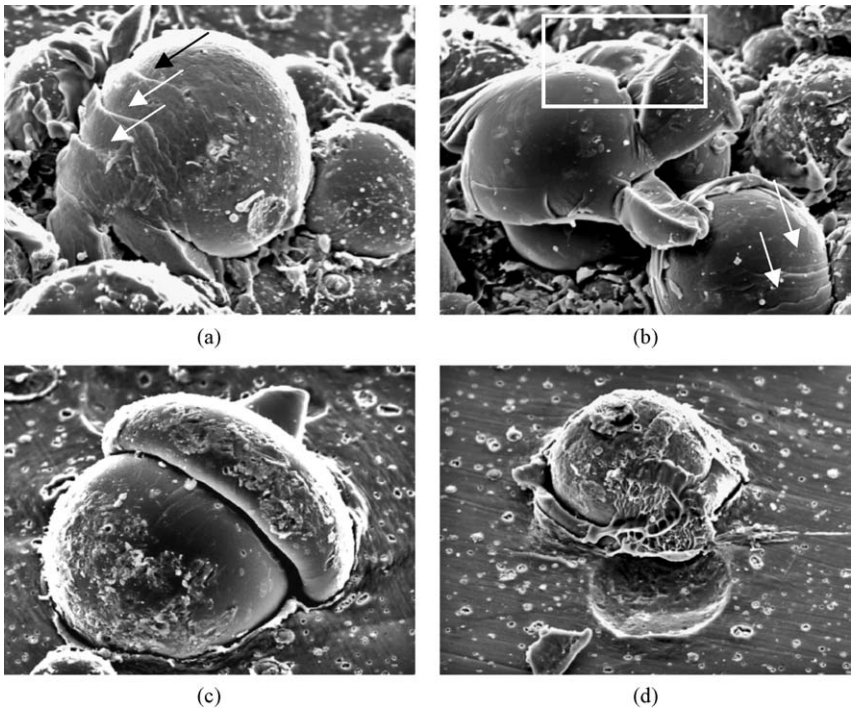

Fig. 6. Characteristic features of a splat deposition onto a splat according to the process gas condition.

hardness and elastic modulus due to high stress during impact. The activation of the shear bands was direct evidence of plasticity during high stress deformation of the bulk metallic glass [17,18]. The shear band angle of the impacted particle on the substrate was close to 48°, as shown in Fig. 7, which was significantly different from 45° for metals that normally occur in a bulk metallic glass [15]. Part C shows the interface melting and viscous flow caused by adiabatic heating during impact.

Heat was generated due to the energy conversion process at the moment of particle impact, and the heat accumulation rate at the impacting interface was affected by heat generation and dissipation rates. In the case of bulk metallic glass, the thermal conductivity is generally low enough to be compatible with ceramic materials [19]. Therefore, heat generation is localized.

When the thermal softening rate was higher than the stress accumulation rate, a sudden transition of the deformation

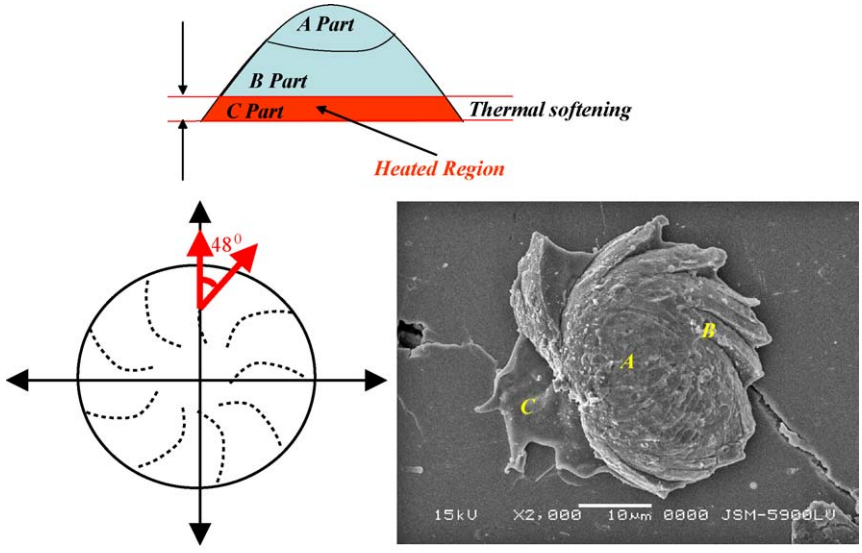

Part A : Little (or no) deformation
Part B : Shear band and fracture
Part C : Melting and viscous flow

Fig. 7. Deposition behavior of BMG particles.

behavior from inhomogeneous deformation to homogeneous deformation was expected. Therefore, plastic deformation between impacting particles and splats resulted in intimate contact. On the other hand, the stress accumulation rate was so rapid that fracture occurred before deformation when the stress accumulation rate was faster than the thermal softening rate. Many factors affect both the thermal softening rate and stress accumulation rate, including the kinetic energy of the impacting particles, pre-existing defects in the splat, and the temperature of both impacting particle and splat.

3.3. Deposition characteristics

Characteristic features of splat morphology of the kinetic sprayed NiTiZrSiSn bulk metallic glass coatings were investigated. In the thermal spraying process, flattening and rapid solidification due to in-pressure and heat transfer at the moment of impact result in mechanical bonding between splats and substrate and between splats. Deposition behavior is, however, quite different in kinetic spraying, because the particles are deposited in the solid-state. In general, severe deformation following the removal of oxide film from the surfaces of impacting particles results in intimate contact with or without melting (as in explosive welding). Therefore, plastic deformation is a key characteristic of kinetic spraying.

In order to verify the thermomechanical properties of NiTiZrSiSn bulk metallic glass, the Vickers microhardness was measured as a function of indentation temperature using a normal load of 400 g of as-sprayed bulk metallic glass coating. Vickers microhardness decreased with increasing indentation temperature and a sharp decrease was observed about 450 °C, as shown in Fig. 8. Consequently, plasticity could be realized during deposition if the particle temperature was increased to near the glass transition temperature at the impacting point.

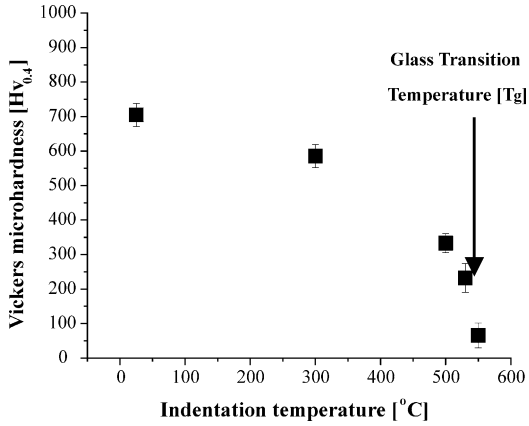

Fig. 8. Variation of Vickers microhardness as a function of indentation temperature.

Coating was overlaid at each process parameter; the cross-sectional morphology is shown in Fig. 9. As can be expected from the individual particle deposition studies, no overlay was obtained when using nitrogen as the working gas. When using helium, the coating thickness was considered to be an indicator of the deposition efficiency, other process parameters being constant. When the carrier gas was heated, not only the coating thickness but also the density was increased, as shown in Figs. 9 and 10. There was no marked difference between the phase composition and thermal properties of the feedstock material and coatings. Therefore, it was hypothesized that both the cooling rate of the molten liquid formed during resolidification and the thermal cycle for the solid-state part of the impacting bulk metallic glass particles in the kinetic spraying process were

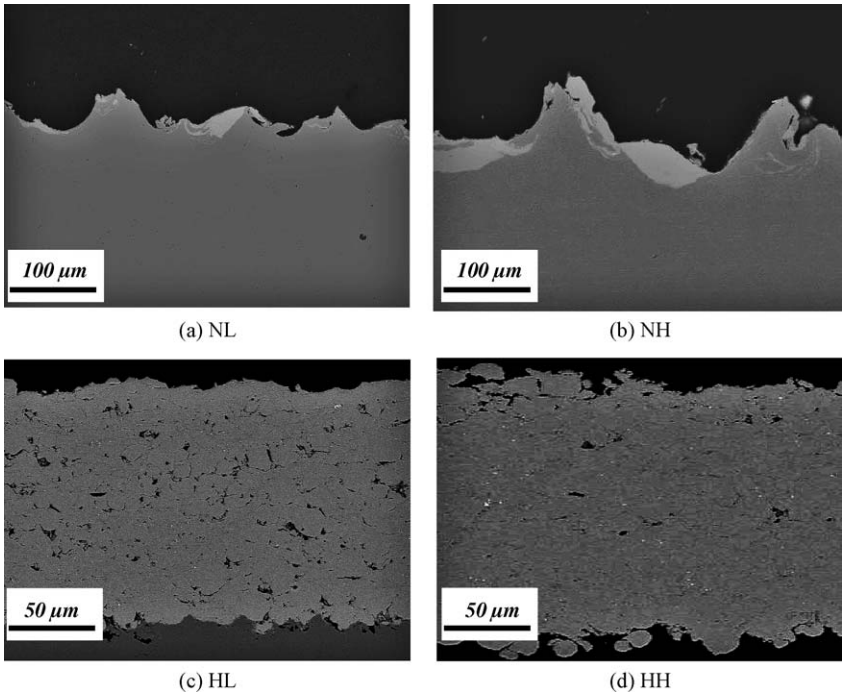

Fig. 9. Microstructures of as-sprayed NiTiZrSiSn bulk metallic glass coatings.

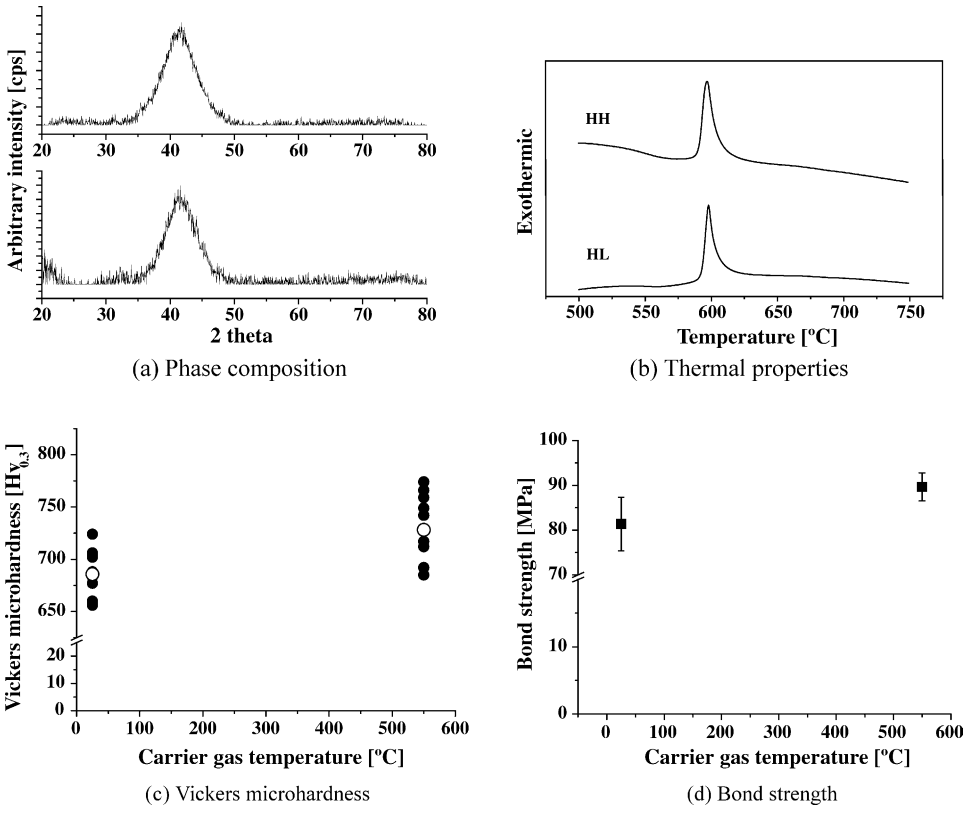

Fig. 10. Characteristics of as-sprayed NiTiZrSiSn coatings.

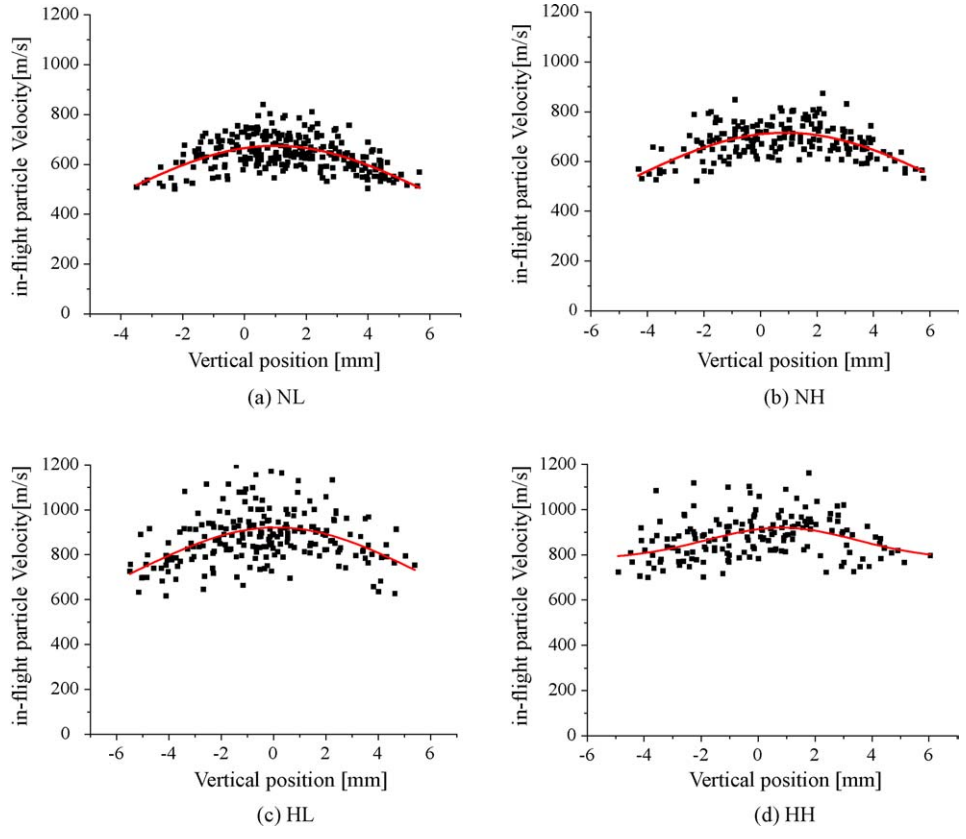

Fig. 11. In-flight NiTiZrSiSn particle velocity.

faster than the critical thermal cycles for crystallization during solidification and reheating. Increases in the Vickers microhardness (Fig. 10c) and bond strength (Fig. 10d) of the coating implied enhanced bonding between splats because the defective microstructures, such as pore and splat boundaries, deteriorate them. These behaviors were consistent with individual particle deposition behavior.

In order to clarify the effects of the process gas species and additional heating on the deposition of bulk metallic glass particles in kinetic spraying, in-flight particle velocity was measured using a SprayWatch at a spraying distance of 30 mm. As shown in Fig. 11, the overall particle velocities were markedly increased by changing the process gas from nitrogen to helium. In addition, the effect of the additional heating of the carrier gas on the particle velocity was negligible though slight data scattering and flattening are observed.

Considering the particle velocity, splat morphology, and coating microstructure, bulk metallic glass particle deposition was primarily dependent on the particle kinetic energy at the impact velocity. Furthermore, the thermal energy resulting from the additional heating helped create intimate contact between particles and splat. It was suggested that the deposition of the elastic bulk metallic glass is determined by the adiabatic heat generation and resulting viscous flow, and the partial melting at the impacting interface following adiabatic shearing on impact.

4. Conclusions

The effects of both process gas species and additional heating on individual particle deposition and resulting coating microstructures have been investigated. By changing the process gas from nitrogen to helium, the deposition efficiency was markedly increased due to the partial melting of the impacting bulk metallic glass particles. Furthermore, the additional heating of the bulk metallic glass particles affected the individual particle deposition behavior and the resulting coating microstructure. Denser coatings were due to the enhancement of the viscous flow of impacting particles, which was enabled by adiabatic shearing when additional heating was applied.

Acknowledgement

This work was financially supported by Ministry of Commerce, Industry and Energy (MOCIE) under the project named “Development of Structural Metallic Materials and Parts with Super Strength and High Performance”.

References

[1] H. Habazaki, T. Sato, A. Kawashima, K. Asami, K. Hashimoto, Mater. Sci. Eng. A 304–306 (2001) 696–700.
[2] X. Wang, I. Yoshii, A. Inoue, Y.H. Kim, I.B. Kim, Mater. Trans. JIM 40 (1999) 1130–1136.
[3] H.J. Lee, E. Akiyama, J. Jabazaki, A. Kawashima, K. Asami, K. Jashimoto, Corros. Sci. 38 (1996) 1269–1279.
[4] T. Gloriant, J. Non-Cryst. Solids 316 (2003) 96–103.
[5] A.L. Greer, Mater. Sci. Eng. A 304–306 (2001) 68–72.
[6] S. Lee, H. Choi, C. Lee, Y. Kim, Mater. Sci. Forum 449–452 (2004) 929–932.
[7] H. Choi, S. Yoon, G. Kim, H. Jo, C. Lee, Scripta Mater. 53 (2005) 125–130.
[8] W.B. Kim, B.J. Ye, S. Yi, Met. Mater. Int. 10 (2004) 1–5.
[9] M.Yu. Gutkin, I.A. Ovid’ko, N.V. Skiba, Acta Mater. 52 (2004) 1711–1720.
[10] W.J. Kim, D.S. Ma, H.G. Jeong, Scripta Mater. 49 (2003) 1067–1073.
[11] J.P. Chu, C.L. Chiang, T.G. Nieh, Y. Kawamura, Intermetallics 10 (2002) 1191–1195.
[12] S. Yi, J.K. Lee, W.T. Kim, J. Non-Cryst. Solids 291 (2001) 132–136.
[13] M. Grujicic, C.L. Zhao, W.S. DeRosset, D. Helfritch, Mater. Des. 25 (2004) 681–688.
[14] M. Heilmaier, J. Mater. Process. Technol. 117 (2001) 374–380.
[15] Z.F. Zhang, J. Eckert, L. Schultz, Acta Mater. 51 (2003) 1167–1179.
[16] T.K. Han, S.J. Kim, Y.S. Yang, A. Inoue, Y.H. Kim, I.B. Kim, Met. Mater. Int. 7 (2001) 91–94.
[17] A.S. Argon, Acta Metall. 27 (1979) 47–58.
[18] A.S. Argon, L.T. Shi, Acta Metall. 31 (1983) 499–507.
[19] M. Yamasaki, Scripta Mater. 53 (2005) 63–67.